tvst

https://doi.org/10.1167/tvst.8.3.22

New Developments in Vision Research

Lenticular Imaging: A New Experimental and Quantitative Analysis of Capsular Dynamics, "Choi-Apple View"

Hyeck Soo Son[1], Ko Un Shin[2], Donghan Kim[3], Patrick Merz[1], Tamer Tandogan[1], Ramin Khoramnia[1], Gerd U. Auffarth[1], Elfriede Friedmann[4], Suehey Chae[5], Kyung Heon Lee[5], and Chul Young Choi[1,2]

[1] The David J. Apple International Laboratory for Ocular Pathology, Department of Ophthalmology, University of Heidelberg, Germany
[2] Department of Ophthalmology, Kangbuk Samsung Hospital, Sungkyunkwan University School of Medicine, Seoul, Republic of Korea
[3] Department of Electrical Engineering, Kyung Hee University, Seoul, Republic of Korea
[4] Institute of Applied Mathematics, University of Heidelberg, Germany
[5] Busan Sungmo Eye Hospital, Busan, Republic of Korea

Correspondence: Chul Young Choi, Department of Ophthalmology, Kangbuk Samsung Hospital, Sungkyunkwan University School of Medicine, Pyeong-dong, Jongno-gu, Seoul, Korea. e-mail: sashimi0@naver.com

Received: 20 September 2018
Accepted: 11 February 2019
Published: 20 May 2019

Keywords: imaging technique; cataract surgery; intraocular lens; lens-zonule dynamics [LZD]; capsular bag dynamics

Citation: Son HS, Shin KU, Kim D, Merz P, Tandogan T, Khoramnia R, Auffarth GU, Friedmann E, Chae S, Lee KH, Choi CY. Lenticular imaging: a new experimental and quantitative analysis of capsular dynamics, "Choi-Apple view". Trans Vis Sci Tech. 2019;8(3):22, https://doi.org/10.1167/tvst.8.3.22

Purpose: Development of a means for quantitative estimation of lenticular and zonular dynamics by using real-time imaging of human autopsy eyes during implantation of different intraocular lens (IOL) models.

Methods: Isolated lenticular structures from human autopsy eyes were prepared in vitro. The following IOLs were implanted: a one-piece C-loop haptic IOL, a three-piece C-loop haptic IOL, and a one-piece plate-type IOL. The amount of deformation of lenticular structures during implantation was calculated and the movements visualized with two cameras. The results were transformed to two-dimensional graphs using a newly developed image-processing algorithm.

Results: For both one-piece plate-type and one-piece C-loop haptic IOLs, the amount of capsular bag deformation from its initial shape was greater in the direction of posterior center of the capsule, as detected by side camera, than in the direction of the equator (or periphery), as detected by front camera. The mean peak deformation values were 51% and 36% (as measured by side and front cameras, respectively) for one-piece plate-type IOL and 25% and 20% for one-piece C-loop haptic IOL. For three-piece C-loop haptic IOL, the capsular bag distention was almost equal in both posterior and peripheral directions, with mean peak deformation values reaching 39% and 38%.

Conclusions: The new experimental means of lenticular imaging and quantified dynamics from two different angles allowed three-dimensional understanding of specific behavior of each IOL. Our model not only exposes the capsular bag for recording during implantation, but also objectively compares the individual movement values and reveals different zonular and capsular stress patterns, depending on IOL model.

Translational Relevance: The novel "Choi-Apple View" allows a three-dimensional quantitative analysis of capsular dynamics and IOL implantation behavior.

Introduction

Lenticular imaging using the Miyake-view has been one of the most popular research tools in ophthalmic imaging studies since 1985.[1] With the development of new imaging techniques, there have also been substantial advances in surgical techniques and intraocular lens (IOL) design. In particular, the "Miyake-Apple" view provides an excellent imaging platform for evaluating the capsular bag dynamics, zonular stress, and surgical manipulations from a unique posterior view—all of which are not readily seen during cataract surgery procedures.[2,3] However, as the Miyake view only allows visual analysis from

the posterior perspective, it fails to take into account the three-dimensional movements of surgical procedures.[4] Despite the proven clinical value of quantifying zonular stress, there are no widespread experimental and clinical methods for simple quantitative detection of the capsular and zonular stress in absolute units.

Therefore, we sought to establish experimentally and clinically viable means for quantitative estimation of lenticular and zonular dynamics from real-time imaging of human autopsy eyes. In this study, we developed lenticular structures of standardized size for analysis and comparison of different IOL models. Two cameras recording the lenticular structures from its side and front helped evaluate the three-dimensional movements of the capsular bag. By measuring the lens-zonule dynamics (LZD) and posterior capsular bag dynamics with real-time images, we applied new imaging techniques and developed a new software[5] that allows translation of mathematical quantification to experimental and clinical settings.

Materials and Methods

Preparation of Isolated Lenticular Structures From Autopsy Eyes

Three human autopsy eyes with intact iris and lens structures were obtained from the Eye Bank of the University of Heidelberg within 72 hours of death and preparation of the globes began immediately after receiving the eyes.

First, the globe was placed on a petri dish with its anterior side facing downward. Using forceps and a 26-G blunt cannula, the globe was manually dissected at its equator. The chorioretinal tissues were separated from the sclera via hydrodissection using saline. The uveal tissues including the iris, lens, ciliary body, and the zonules were then gently separated from the scleral spur. After the isolation of the lenticular structures, every structure was carefully examined via high magnification for any anatomical defects, especially in the zonular and ciliary process area. After trimming the surrounding tissues, we measured the diameter of the isolated structures including the lens and the ciliary processes. Based on the measured value between the distal ends of the ciliary processes, a round hole of 12 mm diameter was made in the central area of a clear plastic plate (45.0 × 45.0 × 0.5 mm in thickness). The isolated lenticular structures were each placed on the plastic plate with the capsular bag protruding through the hole. A second plastic plate of the same size with the same central hole was glued on top of the lenticular structures using superglue to hold and fix them in place. After gently excising the iris near its root using Vannas scissors, capsulorrhexis, open sky cataract extraction, and manual aspiration of the cortical remnants were performed (Supplementary Movie S1).

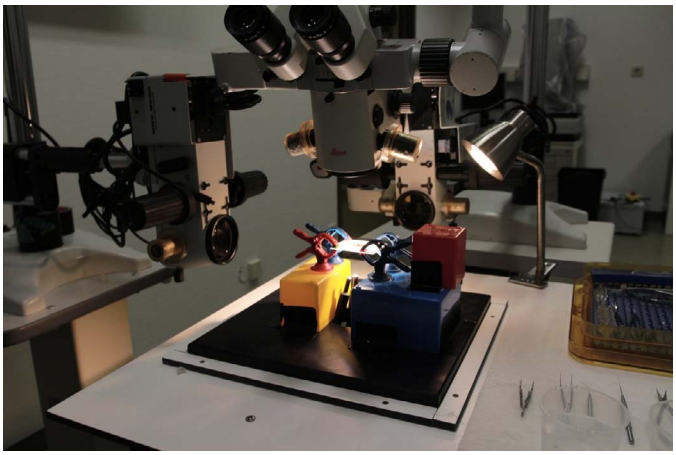

Figure 1. Setup for imaging process. Three operating microscopes were adjusted, and two cameras were placed at side and front of the plate for recording.

Setup for Imaging Process

For simultaneous real-time lateral view recordings, three operating microscopes with recording systems were adjusted horizontal to the plate and mounted such that the first camera viewed the plate from its side (camera A) and the second camera from its front (camera B). A light source from the surgeon's operating microscope and two additional flexible fiber optic light cables were used to illuminate the plate for imaging (Fig. 1). During the recordings, real-time imaging output was used to display the camera view on two different monitors for the assistant. The recording format was ProRes 422, 30 frames per second (FPS), 10 bit, and HD (1920 × 1080) resolution.

Implantation of IOLs Into the Isolated Capsular Bag

The capsular bag was first filled with a sodium-hyaluronate ophthalmic viscoelastic device (OVD) Healon® (Abbott Medical Optics, Santa Ana, CA) that had been stored at room temperature of 21°C, and the initial amount was standardized by checking the height of the capsular structures in the image (distance from the bottom of the plate to the posterior

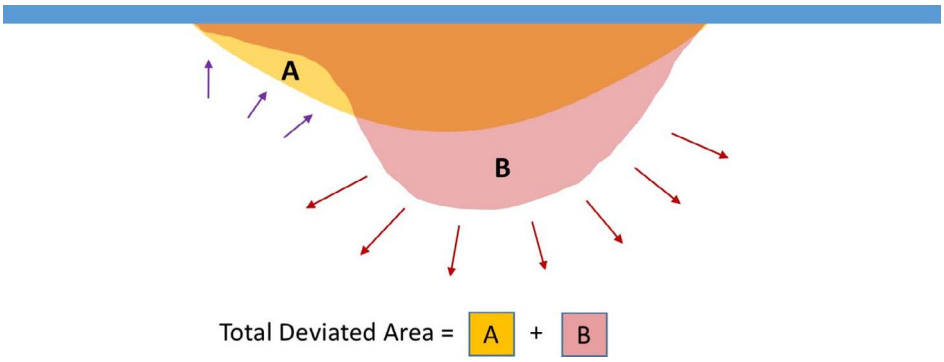

Figure 2. Analyzing the images areas "A" and "B" represent the negative and positive deviations from the initial capsular bag shape, respectively. The summation of A and B represents the total amount of shape deviation at each frame of recording during implantation procedure.

pole of the lens: 3.5 mm). The horizontal size of the capsular images was 10.5 to 11.0 mm. Then, an IOL was injected into the capsular bag using the same method as in conventional cataract surgery. We used three lens models: a one-piece c-looped haptic IOL (IOL 1, AcrySof SA60AT, Monarch III injector with C cartridge; Alcon, Fort Worth, TX), a three-piece c-looped haptic IOL (IOL 2, Sensar AR40e, Emerald injector with C cartridge; Johnson & Johnson, Santa Ana, CA), and a one-piece plate-type IOL (IOL 3, CT Asphina 509MP, Bluemixs™ 180 injector; Carl Zeiss Meditec AG, Jena, Germany). Separate human autopsy eyes were used for each of the three IOL types. All procedures were performed by a single surgeon (C.Y.C.) and recorded simultaneously from two different cameras mounted in two different microscopes at the side and front of the plate.

Analyzing the Images

To analyze and compare the different interactions between the IOL and the capsular bag during the lens implantation, the mathematical group developed a software in C++.[5] With this we calculated the relative deformation values from the original position using real-time imaging (Fig. 2). Area "A" indicates the transformed two-dimensional image recorded by the side camera and area "B" by the front camera. The areas and deviations represent the positive and negative deformation values from the initial shape of the capsular bag. The summation of A and B, therefore, represent the total amount of shape deviation at every frame of recording. The process of converting real-time recordings to two-dimensional image was represented in Supplementary Movie S2, Supplementary Movie S3, and Figure 3. The yellow colored area shows positive deviation and green colored area shows negative deviation from the initial shape of the capsular bag.

All movement values of the lenticular structures during implantation were converted into a graph (Figs. 4, 5, 6) and every peak value represents the maximum deformation value from each time frame of the video. In order to draw an overall comparison and better reflect the realm of each IOL model's implantation behavior, we chose to evaluate among others five peak values and their mean values. Furthermore, the area under the curve was also evaluated as an average value for the entire movement.

Results

Using our anatomical preparation method, we could successfully isolate the lenticular structures with minimal damaging of the adjacent tissues such as lens, capsular bag, iris, and the zonular structures. This method allowed exposure of the lenticular structures for analysis and comparison of movements during implantation of IOLs. Using the developed image-processing algorithm, all recorded images from both (side and front) cameras were analyzed. The evaluation process of the deformation consists of two stages. The first stage includes coloring of the deviation of images from the initial image. The second stage involves the summation of each colored area to compare the real-time results of each IOL implantation. Based on the images captured by the two cameras, we calculated the total deviated area of the capsular bag in pixel units at 30 FPS during the entire implantation duration of approximately 30 to 50 seconds (Fig. 3). It was possible to obtain both overview simplified images and quantification of

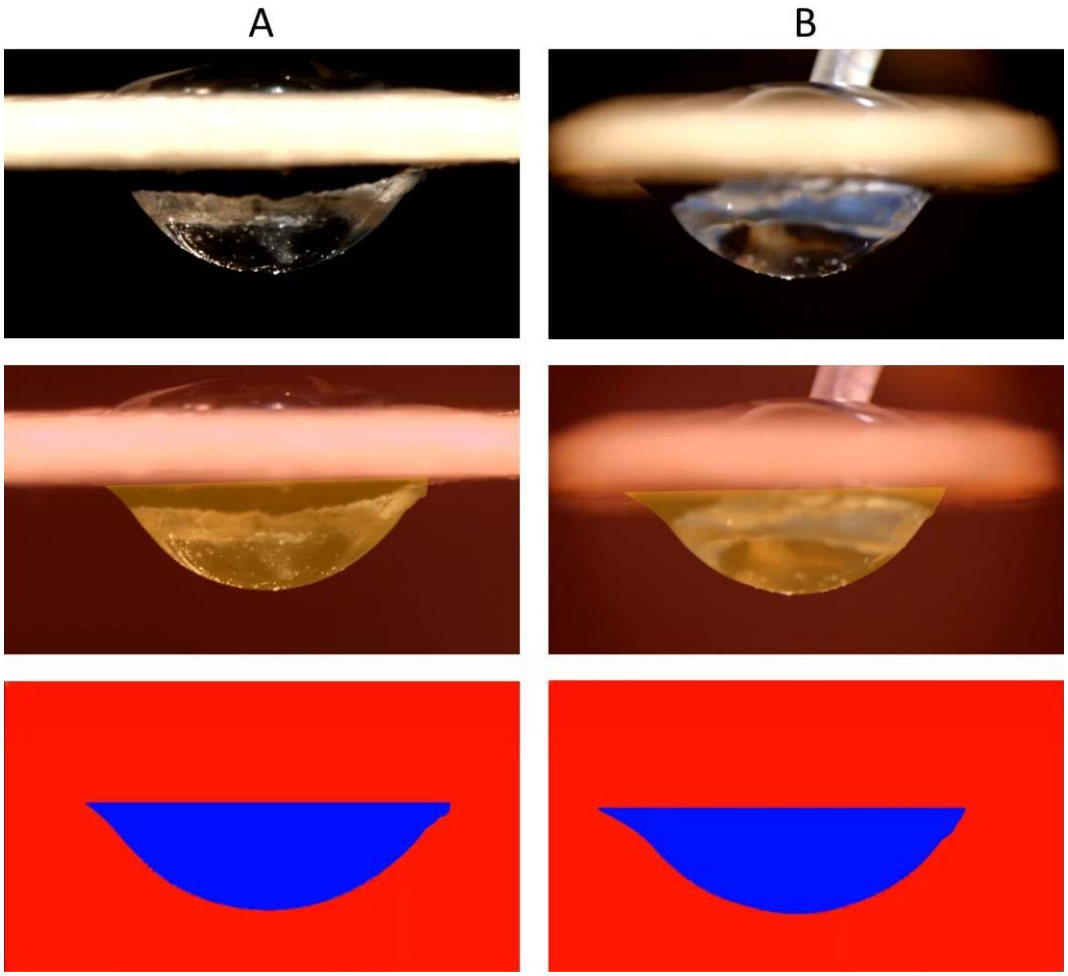

Figure 3. Quantification process of real-time capsular dynamics imaging A and B represent the image at same time frame from side (A) and front (B) camera, respectively. Coded image with three different colors represent the positive (*yellow color*) and negative (*green color*) deviation from original setup.

posterior capsular bag dynamics during IOL implantation.

Figures 4, 5, and 6 show the graphs of real-time movements of IOL 1, IOL 2, and IOL 3 implantation, respectively. For each graph, five peak values detected by cameras A and B (A1-5, B1-5) during the implantation process were marked and their average values calculated, allowing analysis of moments of maximum deformation, amount of average deformation, as well as extent of total deformation of lenticular structures. The detected peaks and their mean values are summarized in the Table and illustrated in Figure 7 for graphic comparison.

One-Piece C-Loop Haptic IOL (Fig. 4)

For the one-piece C-loop haptic lens, it is evident that the IOL implantation process was largely divided into two separate parts: the first part corresponding to the delivery of the IOL itself and the second part corresponding to the movements during IOL positioning in the capsular bag. All peak values were captured during the first part of the implantation, except for one peak (A3) that was measured during the latter. Throughout the entire time sequence, the capsular distention values measured by the side camera A were higher than those measured by the front camera B, as reflected by the measured mean peak values of 25% (camera A; range: 34%–20%) and 20% (camera B; range: 22%–17%).

Three-Piece C-Loop Haptic IOL (Fig. 5)

The three-piece C-loop haptic lens showed similar implantation behavior as the one-piece C-loop haptic lens, with two separate moments of movements: the delivery of the IOL and the lens positioning. All peak

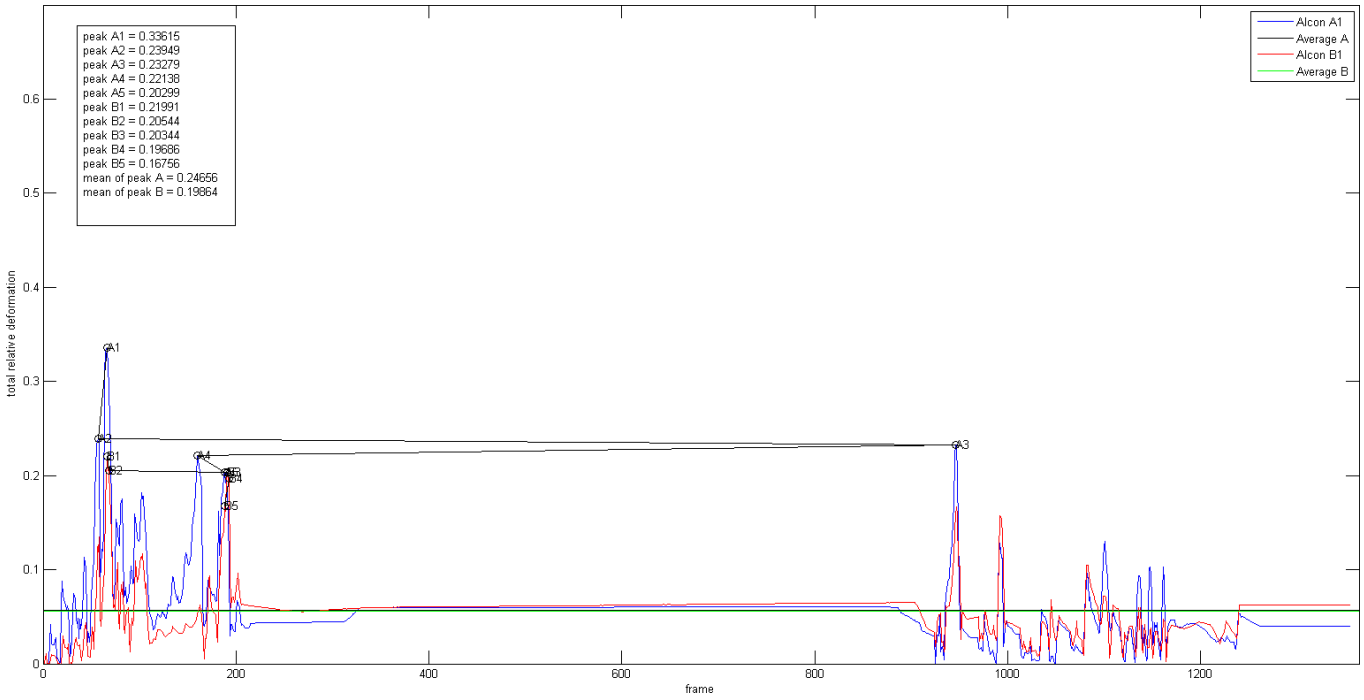

Figure 4. Real-time graphs during the period of IOL 1 implantation one-piece C-loop haptic IOL (IOL 1, AcrySof SA60AT, Monarch III injector with C cartridge, Alcon).

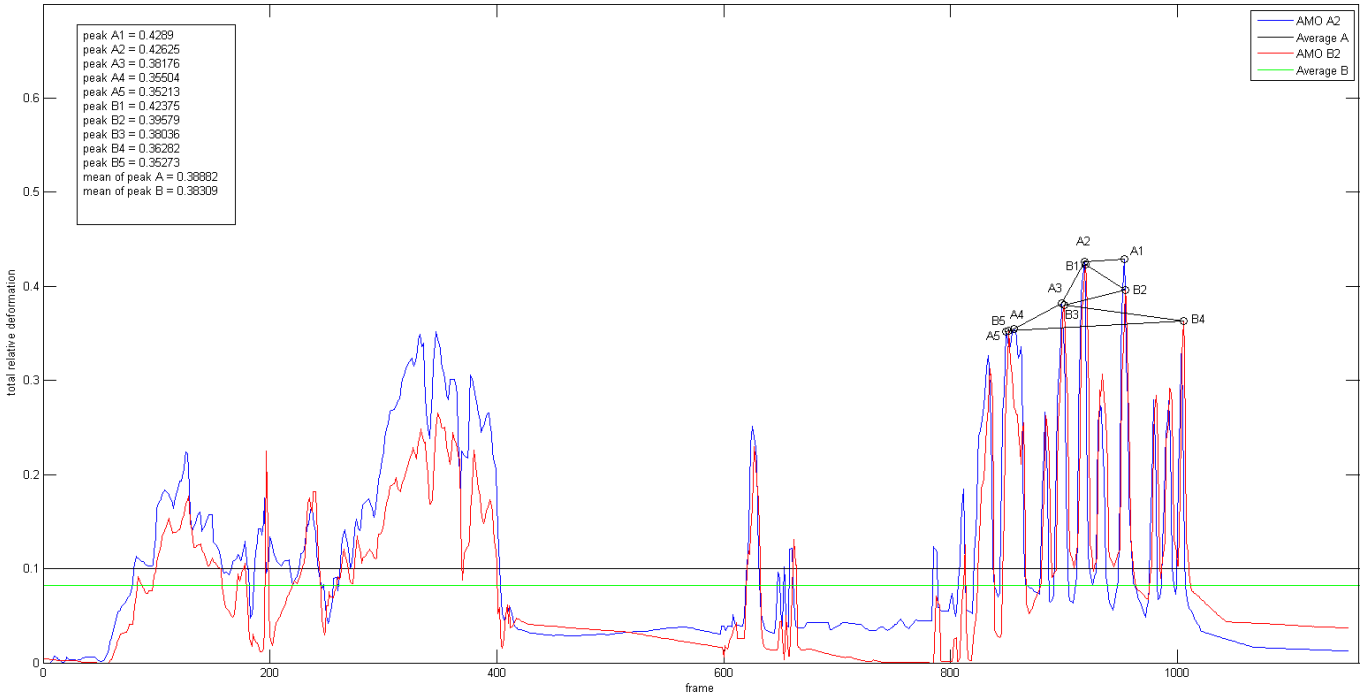

Figure 5. Real-time graphs during period of IOL 2 implantation three-piece C-loop haptic IOL (IOL 2, Sensar AR40e, AMO, Emerald injector with C cartridge).

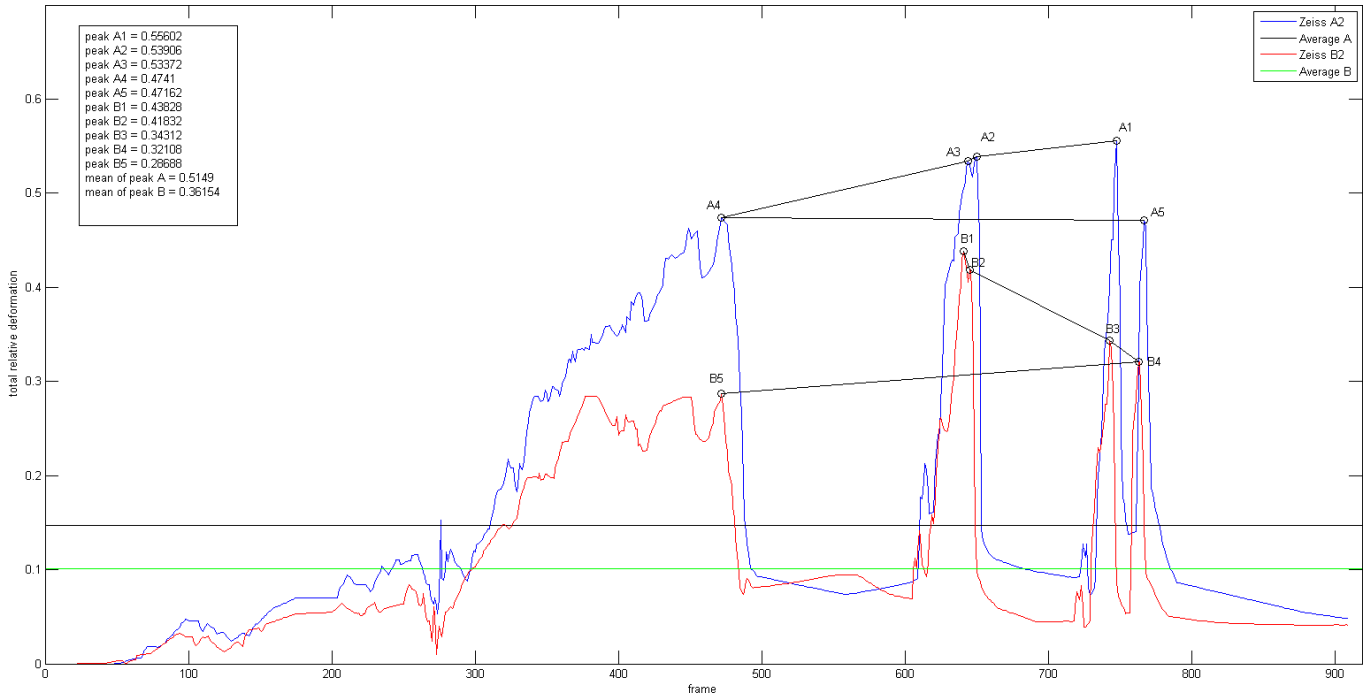

Figure 6. Real-time graphs during period of IOL 3 implantation one-piece plate-type IOL (IOL 3, CT Asphina 509MP, Bluemixs 180 injector, Zeiss).

values were greater than those measured in the one-piece C-loop lens and were observed while positioning the IOL, with mean peak values of 39% from camera A (range: 43%–35%) and 38% from camera B (range: 42%–35%). The peak values measured by the two cameras were very similar during the IOL positioning. During the delivery of the IOL, however, the amount of capsular distention captured by the side camera was higher than that captured by the front camera, suggesting the impact of insertion vector that led to lenticular structures distending more in the direction of the IOL injection.

One-Piece Plate-Type IOL (Fig. 6)

In comparison to the other two IOL types, the one-piece plate-type IOL demonstrated the highest deformation values, with mean peak values of 51% (range: 56%–47%) and 36% (range: 44%–29%) from cameras A and B, respectively. Clearly, the side camera detected more movements than the front camera, once again indicating the impact of insertion vector for this type of IOL as well. Furthermore, in contrast to the other IOLs, this plate-type IOL showed a wider distribution of peak values and a rather merged crescendo-decrescendo deformation behavior.

Table. Overview of the Measured Peak Movement Values and Their Average Values for Each IOL Type as Measured by Cameras A and B

	One-Piece C-Loop Haptic IOL		Three-Piece C-Loop Haptic IOL		One-Piece Plate Haptic IOL	
	Peak Values		Peak Values		Peak Values	
	Side (A)	Front (B)	Side (A)	Front (B)	Side (A)	Front (B)
1	34%	22%	43%	42%	56%	44%
2	24%	21%	43%	40%	54%	42%
3	23%	20%	38%	38%	53%	34%
4	22%	20%	36%	36%	47%	32%
5	20%	17%	35%	35%	47%	29%
Mean	25%	20%	39%	38%	51%	36%

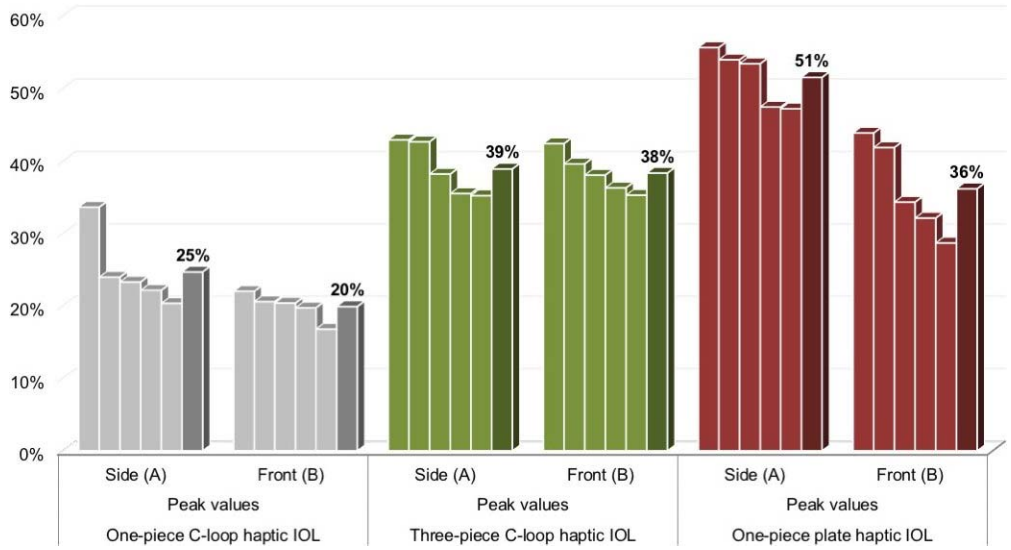

Figure 7. Comparison of the peak movement values and their mean values between three different IOL types.

Discussion

Significant enhancements in cataract surgical techniques and implant technology have been achieved from cadaver eye studies, ranging from basic improvements in lens fixation[5] to advances in managing the posterior capsular bag.

In 1985, Miyake and Miyake[1] published a study of IOL haptic fixation in which they implemented a technique of posterior cinematography using a 16-mm camera in enucleated human autopsy eyes. The significant advance of this study was that the technique allowed simultaneous anterior view and posterior cinematography of the anterior segment while surgery was being performed. In 1990, the method was modified by Apple et al.,[6] who improved the equipment and globe preparation technique to allow real-time viewing and high-resolution capability together with enhanced magnification. The Miyake-Apple technique provides a unique view of both the anterior segment structures and the surgical manipulations and is particularly useful in the evaluation of the capsular bag dynamics and zonular stress, the inner surface of the iris, ciliary processes, and the anterior vitreous face, that are not readily seen during surgical procedures or by clinical inspection. However, as only the posterior view was available, previous studies could only show two-dimensional images of the capsular bag,[7–10] not allowing a three-dimensional movement analysis of the capsular dynamics. Also, previous studies merely viewed the recorded images and could not analyze the images quantitatively.[7–10]

In this study, we present a new experimental technique for analyzing the posterior capsular bag dynamics during IOL implantation. With a newly developed software, quantification and comparison of different IOL types was made possible. This is the first study in this application in which real-time two-dimensional images were converted to a mathematical graph to visualize the dynamics quantitatively.

Using our experimental model and software, we could evaluate each characteristic behavior of different IOLs during implantation by evaluating the dynamics including peak movement and average deviation of the capsular bag. Also, a reproducible model with standardized size minimized the variation in results. We expect that our model can be applied in other studies of capsular dynamics.

Our results in this study showed different dynamic patterns for the studied IOLs. The one-piece plate-type IOL demonstrated the highest mean peak values of capsular deformation and the magnitude of distention was much larger in the posterior direction, as captured by the side camera, than that in peripheral direction, as captured by the front camera, suggesting a dominantly one-vectoral movement of the implantation of this IOL type. Similarly, the one-piece C-loop haptic IOL also showed a greater capsular deformation in the posterior direction, but its mean peak values of capsular deformation were much lower in comparison to the other two IOL types. Also, its implantation time sequence involved two separate moments of movements, namely the delivery of the

IOL itself and the subsequent IOL positioning. The peak movement values were, however, comparable in both parts. The three-piece C-loop haptic IOL exhibited a similar pattern as well, yet their mean peak values were higher than those of the one-piece C-loop haptic IOL, and their peak movement values in both posterior and peripheral directions were almost identical during the IOL positioning process. These results need to be clarified via statistical analyses with more human autopsy eyes.

This technique could contribute to the development of new improved IOLs or ocular implants in addition to better surgical techniques, not only for cataract surgery, but also for other ocular surgeries. Furthermore, it is also applicable for studying the capsular and zonular interactions during the delivery of new types of IOLs and different capsular tension rings. Moreover, the potential influence of insertion vector on the differences in the peak value patterns of each IOL type also could unveil new modalities for implantation techniques to reduce intraoperative stress on ocular tissues.

There are several limitations in this study. First, as we obtained the results from prepared autopsy eyes that differed in their characteristics and composition from eyes in vivo, clinical situations should be considered before applying the results. Secondly, although the presence of surrounding anatomical structures such as the anterior chamber, the sclera, and the posterior vitreous support could lead to different results, the approach in this study is designed to only analyze the magnitude of zonular and capsular dynamics, minimizing the influence of any other factors. The lack of vitreous support in our model may lead to an exaggeration of the capsular movements during the implantation of the IOLs. Future studies utilizing this imaging technique in an artificial anterior segment may also be useful in better simulating the clinical situation as a variety of variables such as angle of approach, area of initial contact of the capsule, etc., may be tested under a more controlled setting. Furthermore, even though we recorded two-dimensional images with two different cameras, we cannot obtain the real three-dimensional capsular volume changes directly. In most cases, each isolated capsular structure was not stable or rigid enough to perform the IOL implantation more than three to five times. In addition, the interactions between the IOLs and the OVDs used in this study should also be considered when interpreting the results.

Conclusions

As a result of continuous progresses in anatomical approaches, imaging techniques, and applied mathematics, quantification of real-time interactive dynamics between the zonules and the capsular bag during IOL implantation has become possible. Our new experimental lenticular imaging technique together with the newly developed software allowed the quantification of capsular movements from two different angles, providing a three-dimensional understanding of the specific behavior of each IOL. This novel imaging and analysis system will aid further experimental research to investigate the lenticular dynamics.

Acknowledgments

Donald J. Munro contributed to the review of the pre-publication report.

Supported by Medical Research Funds from Kangbuk Samsung Hospital, Busan Sungmo Eye Hospital sodam Scholarship Committee, and Klaus Tschira Foundation GmbH, Heidelberg, Germany, project 00.265.2015.

Disclosure: **H.S. Son**, None; **K.U. Shin**, None; **D. Kim**, None; **P. Merz**, None; **T. Tandogan**, None; **R. Khoramnia**, None; **G.U. Auffarth**, None; **E. Friedmann**, None; **S. Chae**, None; **K.H. Lee**, None; **C.Y. Choi**, None

References

1. Miyake K, Miyake C. Intraoperative posterior chamber lens haptic fixation in the human cadaver eye. *Ophthalmic Surg*. 1985;16:230–236.
2. Ahmed II, Cionni RJ, Kranemann C, Crandall AS. Optimal timing of capsular tension ring implantation: Miyake-Apple video analysis. *J Cataract Refract Surg*. 2005;31:1809–1813.
3. Werner L, Hickman MS, LeBoyer RM, Mamalis N. Experimental evaluation of the Corneal Concept 360 intraocular lens with the Miyake-Apple view. *J Cataract Refract Surg*. 2005;31:1231–1237.
4. Pereira FA, Werner L, Milverton EJ, Coroneo MT. Miyake-Apple posterior video analysis/

photographic technique. *J Cataract Refract Surg*. 2009;35:577–587.
5. Friedmann E, Siekmann T. DeformCaB, C++ Software which quantifies the capsular bag deformation during intraocular lens (IOL) implantation. https://ganymed.math.uni-heidelberg.de/~elfi/. Accessed on May 13, 2019.
6. Apple DJ, Lim ES, Morgan RC, et al. Preparation and study of human eyes obtained postmortem with the Miyake posterior photographic technique. *Ophthalmology*. 1990;97:810–816.
7. Davis BL, Nilson CD, Mamalis N. Revised Miyake-Apple technique for postmortem eye preparation. *J Cataract Refract Surg*. 2004;30:546–549.
8. Auffarth GU, Wesendahl TA, Solomon KD, et al. A modified preparation technique for closed-system ocular surgery of human eyes obtained postmortem: an improved research and teaching tool. *Ophthalmology*. 1996;103:977–982.
9. Assia EI, Apple DJ. Side-view analysis of the lens. I. The crystalline lens and the evacuated bag. *Arch Ophthalmol*. 1992;110:89–93.
10. Assia EI, Apple DJ. Side-view analysis of the lens. II. Positioning of intraocular lenses. *Arch Ophthalmol*. 1992;110:94–97.

Supplementary Material

Supplementary Movie S1. Preparation process of isolated lenticular structures.

Supplementary Movie S2. Real-time lenticular structure dynamics in the original video.

Supplementary Movie S3. Real-time lenticular structure dynamics converted to a two-dimensional image. The *yellow colored area* shows positive deviation, and the *green colored area* shows negative deviation from the initial shape of the capsular bag.